Materials Research Proceedings 28 (2023) 1759-1764 https://doi.org/10.21741/9781644902479-190

Modeling electrochemical machining based on effective parameters

WAIMANN Johanna[1,2,a *], VAN DER VELDEN Tim[2,b], SCHMIDT Annika[2,c], RITZERT Stephan[2,d] and REESE Stefanie[2,e]

[1] Modeling and simulation techniques for systems of polycrystalline materials, RWTH Aachen University, Mies-van-der-Rohe-Str. 1, 52074 Aachen, Germany

[2] Institute of Applied Mechanics, RWTH Aachen University, Mies-van-der-Rohe-Str. 1, 52074 Aachen, Germany

[a]waimann@ifam.rwth-aachen.de, [b]vandervelden@ifam.rwth-aachen.de, [c]schmidt@ifam.rwth-aachen.de, [d]ritzert@ifam.rwth-aachen.de, [e]reese@ifam.rwth-aachen.de

Keywords: Electrochemical Machining, Effective Parameters, Material Modeling, Finite Element Method

Abstract. The process of electrochemical machining uses chemical reactions to dissolve material of the surface layer. This special kind of processing avoids undesired microstructural changes in the surface, such as the formation of dislocations. ECM is thus a very promising processing technique for high-strength materials. To model the complex chemical reactions in a computationally efficient manner, an inner variable is introduced, which describes the dissolution level of the material. The evolution of the inner variable is formulated based on Faraday's law of electrolysis. Furthermore, the use of an effective formulation of the necessary material parameters enables to consider this homogenized description of the dissolution process within an electrical finite element framework. Each effective material parameter is a result of classical mixture rules.

Introduction

Electrochemical machining (ECM) takes advantage of the anodic dissolution of metals, see exemplary in [1]. Due to the absence of mechanical loads during the ECM process, no undesired side effects, like formation of dislocations or residual stresses, occur. It is thus also possible to process even high-strength materials, see for instance [2-5].

The chemical reaction is driven by the electrochemical potential, whereby compared to electropolishing the electric part of the potential – and not the chemical one – is dominant. Fig. 1 schematically shows the idea of the process. The work piece and the tool serve as anode and cathode in the electrically loaded system. Due to the contact with the electrolyte and the already mentioned electrochemical potential the effect of the anodic dissolution takes place. This means that the metallic material depending on its valence dissolves into electrons, which go to the anode, and metal ions that are flushed away by the fluid. In reality – of course – the reactions are much more complicated, for instance due to a developing oxide layer, which would delay the dissolution process, as well as due to reactions at the cathode. The authors propose a new strategy [6], which is kept simple for the beginning and will be further extended step by step in future works. For the consideration of the oxide layer's influence on the dissolution of the work piece, a first approach is proposed in this article.

The next two sections deal with the generalized modeling concept using a smoother description of the dissolution as well as the related evolution equations. The idea has been already introduced in [6]. In the following, an introduced flow function enables to consider the influence of the already mentioned oxide layer. The article is completed by two simulations and conclusions in the later sections, respectively.

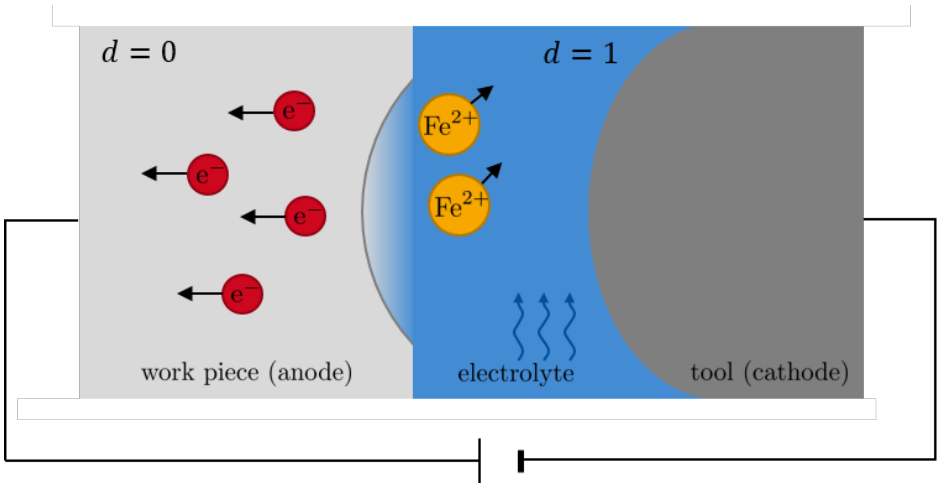

Fig. 1. Concept of the dissolution process with iron-based dissolution, see also [6,7]: dissolution variable $\boldsymbol{d}$ *varying between* $\boldsymbol{d = 0}$ *in the metal and* $\boldsymbol{d = 1}$ *in the electrolyte.*

The Concept of Effective Parameters Using the Dissolution Level as an Inner Variable

The inner variable d describes the state of the dissolution process. Hence, it is zero for the undissolved metal material and one for the completely dissolved material and thus for the electrolyte. At this point, for simplicity, the assumption is made, that the metal ions are permanently removed by the fluid flow. During the chemical reaction, d ranges between zero and one. Each material parameter at each material point within the simulation is then determined using a classical mixture rule. The resulting effective parameters are then marked by $\overline{(\cdot)}$. Depending on the choice of a series or parallel connection, they have one of the following forms

$$\overline{(\cdot)}_S = \left[(1-d)\frac{1}{(\cdot)^{ME}} + d\,\frac{1}{(\cdot)^{EL}}\right]^{-1} \tag{1}$$

$$\overline{(\cdot)}_P = (1-d)(\cdot)^{ME} + d\,(\cdot)^{EL} \tag{2}$$

respectively. Therein, $(\cdot)^{ME}$ and $(\cdot)^{EL}$ correspond to the individual material parameters of the metal and the electrolyte.

The conservation of electric charge that describes the electrical part of the observed multiphysical problem reads

$$\dot{\rho}_E + \mathrm{div}(\boldsymbol{j}) = 0 \tag{3}$$

wherein, the charge density ρ_E and the current density $\boldsymbol{j}$ depend on the field strength $\boldsymbol{E}$. They have the following forms

$$\rho_E = \mathrm{div}(\epsilon_0\,\bar{\epsilon}_r(d)\,\boldsymbol{E}) \tag{4}$$

$$\boldsymbol{j} = \bar{\kappa}_E(d)\,\boldsymbol{E} \tag{5}$$

with the material related and based on Eq. 1 or 2 effectively chosen relative permittivity $\bar{\epsilon}_r(d)$ and electric conductivity $\bar{\kappa}_E(d)$, the electric constant ϵ_0 as well as $\boldsymbol{E}$.

The primary unknown of the electrical problem is the electric potential v. Not yet obvious in the presented equations, its gradient is considered within the electric field strength via

$$\boldsymbol{E} = -\mathrm{grad}(v) \tag{6}$$

The original paper [6] additionally considers a thermally coupled system. There also a more detailed description of the effective parameter approach can be found, which is also later used for the consideration of a relocatable cathode in terms of a moving boundary value problem [7]. Due to simplicity, the additional thermal problem is skipped, here. More information on the finite element formulation and implementation can be found in [6,8].

Evolution of the Dissolution Level Based on Faraday

The anodic dissolution leads to the split of a metal atom into electrons and ions, see also Fig. 1. The temporal amount of the dissolution by this reaction can be described by Faraday's law of electrolysis. Motivated by [9] and introduced in [6,7], one can formulate the evolution equation of the inner variable d. The dissolution level of an incremental reference volume $\mathrm{d}V_{ref}$ reads

$$\dot{d}\ \mathrm{d}V_{ref} = v_{dis}\ \mathcal{A}\ \mathrm{d}I. \tag{7}$$

In Eq. 7, v_{dis} is a material parameter which is experimentally observed by our project partners of the *Werkzeugmaschinenlabor (WZL)* at RWTH Aachen University. It is thus not only related to Faraday's law but also to the efficiency of the performed experiment. The quantity $\mathrm{d}I$ describes the increment of the electric current. Furthermore, the dissolution only takes place if the material has contact to the electrolyte. To account for this constraint, the activation function $\mathcal{A}$ is introduced. The latter becomes one for contact with the electrolyte and is otherwise zero. This ensures that the anodic dissolution only takes place in material layers, which are at the surface.

Consideration of a Formed Oxide Layer and Its Damping Properties

The former sections deal with the state of the art of the new method to describe the ECM process. In the following, the modeling approach is extended to consider the oxide layer formation in dependency on $\boldsymbol{j}$. During the ECM process, one can observe the formation of such a layer on the anodic surface (see Fig. 2), which shows a diode-like influence on the electric problem and, thus, serves with the polarization voltage Δv_p as a barrier that has to be overcome before the dissolution process in the trans-passive regime can start.

The considered modeling strategy to methodologically describe the ECM process, was - due to our origin in mechanics - always driven by the idea of applying general solution schemes of mechanical problems to the electrochemical one. The presented work focuses on the more dominant trans-passive area and for simplicity neglects the removal at low current densities before the passivation of the material. Following the characteristics of a yield function in plasticity, a flow function ϕ^{OX} is introduced. As long as $\phi^{OX} \leq 0$, the oxide layer serves as an isolating barrier, preventing the electric flow. When $\phi^{OX} > 0$, the current flow over the surface as well as the dissolution process are initiated. A first assumption for a one-dimensional formulation of ϕ^{OX} reads:

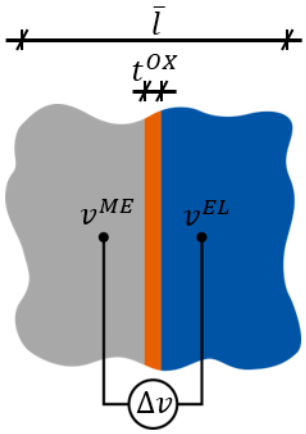

Fig. 2. Unit cell for the surface area with a characteristic length $\bar{\boldsymbol{l}}$: metal (grey) with potential $\boldsymbol{v^{ME}}$, oxide layer (orange) with thickness $\boldsymbol{t^{OX}}$ and electrolyte (blue) with potential $\boldsymbol{v^{EL}}$.

$$\phi^{OX} = |\boldsymbol{v}^{ME} - \boldsymbol{v}^{EL}| - \Delta v_p = \begin{cases} \leq 0 : \text{insulating} \\ > 0 : \text{conducting} \end{cases} \tag{8}$$

The choice of the flow function is based on experimental observations. The electric flow through the oxide layer and, thus, the material dissolution can start when the flow function is positive. Physically, this means that the potential difference

$$\Delta v = |v^{ME} - v^{EL}| \tag{9}$$

is higher than the polarization voltage Δv_p. For the three-dimensional case the formulation of a flow function is much more complicated. The reason for that is that one has to check the potential difference in each direction, especially for curved surfaces. But, this formulation is part of our future works.

Furthermore, the existence of the oxide layer also influences the effective material parameters. According to the chosen approaches in Eq. 1 and 2, they read

$$\overline{(\cdot)}_S = \left[(1-d)\frac{1}{(\cdot)^{ME}} + \frac{t^{OX}}{\bar{l}}\frac{1}{(\cdot)^{OX}} + d\frac{1}{(\cdot)^{EL}}\right]^{-1} \tag{10}$$

$$\overline{(\cdot)}_P = (1-d)(\cdot)^{ME} + \frac{t^{OX}}{\bar{l}}(\cdot)^{OX} + d\,(\cdot)^{EL} \tag{11}$$

Therein, $(\cdot)^{OX}$ corresponds to the parameters of the oxide layer, which are weighted by its thickness t^{OX} in relation to the effective length $\bar{l}$ of the examined unit cell.

Finally, the introduction of a modified current density $\boldsymbol{j}_{mod}$ enables to take into account the insulating character of the oxide layer. It has the form:

$$\boldsymbol{j}_{mod} = \begin{cases} \boldsymbol{0}, & \phi^{OX} \leq 0 \\ \boldsymbol{j} - j_0\boldsymbol{n}, & \phi^{OX} > 0 \end{cases} \tag{12}$$

with the normal $\boldsymbol{n}$ on the metal surface and a reduction term

$$j_0 = \kappa_E^{OX}\left(-\frac{\Delta v_p}{t^{OX}}\right) \tag{13}$$

Numerical Results

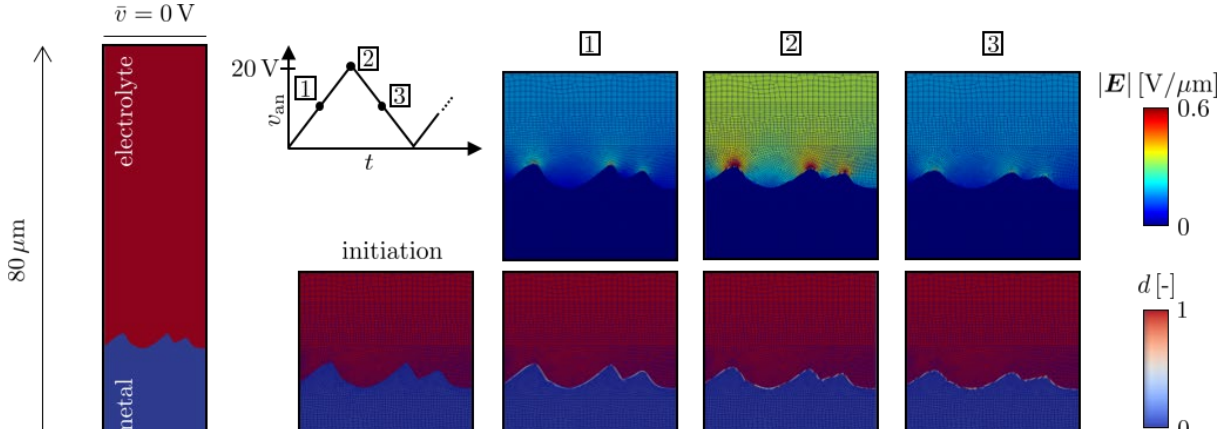

Fig. 3. Pulsed electrochemical machining with initial non-uniform roughness and without consideration of the oxide layer: boundary value problem (left) as well as norm of the electric field strength $\boldsymbol{E}$ and dissolution level $\boldsymbol{d}$ for different load steps during the first cycle (right).

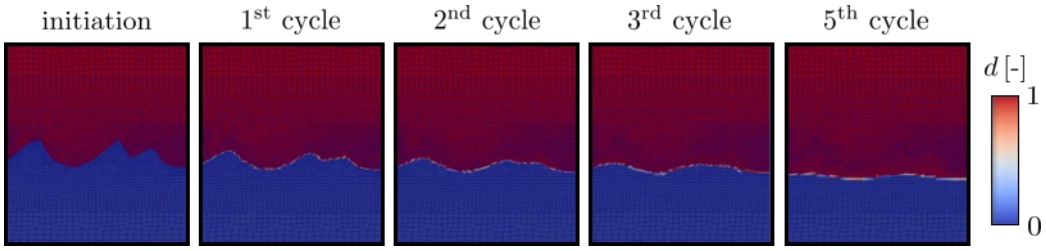

Fig. 4. Pulsed electrochemical machining with initial non-uniform roughness and without consideration of the oxide layer: dissolution level $\boldsymbol{d}$ *after individual load cycles.*

Within this chapter, two simulations are presented. The used material parameters are given in [6]. The first example shows the simulation of a pulsed electrochemical processing of a material surface with an initial non-uniform roughness and without considering the influence of the oxide layer. Fig. 3 (*left*) shows the boundary value problem. The electric potential is prescribed at the anode and linearly varied between 0 V and 20 V. It is zero at the cathode. On the right part of Fig. 3, the norm of the electric field strength and the dissolution level for different time steps of the first pulse are presented: The electric field strength is highest at the peaks of the structure and results in a faster dissolution, there. The flattening of the surface roughness is also presented in Fig. 4. It shows the dissolution level before the first, after the first, second, third and fifth cycle. Similar simulations with a different initial roughness are also given in [6] and [10].

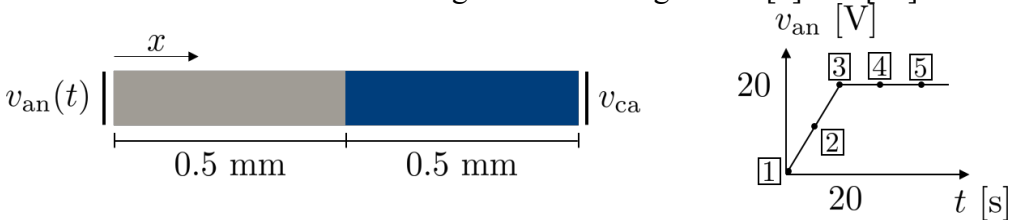

Fig. 5. Electrochemical machining with consideration of the oxide layer: boundary value problem (left) and prescribed electric potential at the anode with marked load steps (right).

In the second example, a one-dimensional academic problem is assumed as presented in Fig. 5. The electric potential at the cathode is prescribed with zero. At the anode the potential is linearly increased to a maximum value of 20 V and then kept constant. The assumed polarization voltage reads $\Delta v_p = 1.5$ V. Fig. 6 shows the resulting dissolution level and the electric potential for some chosen times steps, which are marked in Fig. 5. The results for this first simulation considering the oxide layer show that before the difference between the electric potential in the metal and the electrolyte reaches the critical value of the polarization voltage no material dissolution takes place. After that, the chemical reaction is initiated and the dissolution begins.

Summary

The presented model contributes to the field of modeling the anodic dissolution during electrochemical machining. The formulation is based on the use of effective material parameters.

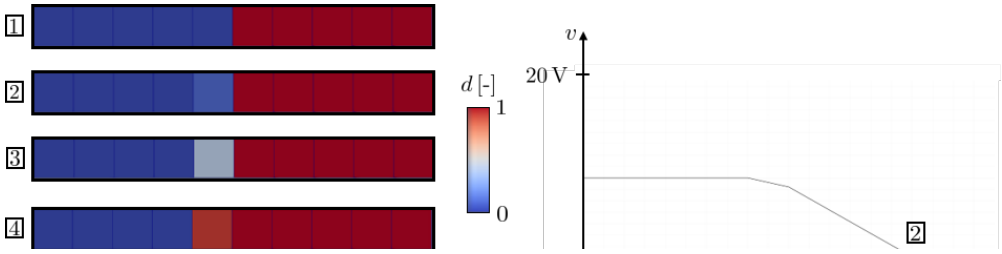

Fig. 6. Electrochemical machining with consideration of the oxide layer: dissolution level $\boldsymbol{d}$ *(left) and electric potential* $\boldsymbol{v}$ *plotted over* $\boldsymbol{x}$ *(right) at marked load steps, see Fig. 5.*

Compared to our earlier works, an idea is proposed how the influence of a formed oxide layer can be taken into account and which thus refers to the trans-passive area of the electrochemical process. The presented numerical results reveal the complex mechanism.

The earlier described material model already accounts for the iron-based dissolution based on Faraday's law of electrolysis. Now, the model also accounts for a polarization voltage which has to be overcome within the trans-passive area, before the removal can start. But, of course, it is still a simplification of the complex and coupled chemical reactions. Besides further three dimensional simulations of the ECM process – also in combination with the removal before passivation – in future works, the modelling approach must be able to consider the full electrochemical potential to describe the material dissolution of the individual alloying elements at the anode. Additionally, a polycrystalline structure and different phases of the metal will be included, which influence the resulting surface roughness. Once the reactions at the anode will be described in more detail, the focus of further works will lie on the reactions at the cathode and the fluid structure interaction. The presented model neglects these local effects on the dissolution process and assumes, so far, that developed heat, gases and ions are permanently transported away by the electrolyte.

Acknowledgements
The authors gratefully acknowledge the financial support of the German Research Foundation (DFG, Deutsche Forschungsgemeinschaft) within the transregional Collaborative Research Center SFB/TRR 136, project number 223500200, subproject M05. We also kindly acknowledge our project partners of the Werkzeugmaschinenlabor (WZL) and the Chair of Corrosion and Corrosion Protection (KKS) at the RWTH Aachen University for many interesting and helpful discussions on the ECM process and the chemical reactions as well as for the essential experimental support.

References
[1] C.H. Hamann, W. Vielstich, Electrochemistry, 3. tot. rev. and enl. ed., Wiley-VCH, Weinheim, 1998.
[2] F. Klocke, A. Klink, D. Veselovac, D.K. Aspinwall, S.L. Soo, M. Schmidt, J. Schilp, G. Levy, J.-P. Kruth, Turbomachinery component manufacture by application of electrochemical, electro-physical and photonic processes, CIRP Ann. - Manuf. Technol. 63 (2014) 703-726. https://doi.org/10.1016/j.cirp.2014.05.004
[3] A.E. DeBarr, D.A. Oliver, Electrochemical Machining, Macdonald & Co., Ltd, London, 1968.
[4] J.A. McGeough, Principles of Electrochemical Machining, first ed., Chapman & Hall, London, 1974. https://doi.org/10.1002/cite.330472314
[5] T. Bergs, S. Harst, Development of a process signature for electrochemical Machining, CIRP Ann. - Manuf. Technol. 69 (2020) 153-156. https://doi.org/10.1016/j.cirp.2020.04.078
[6] T. van der Velden, B. Rommes, A. Klink, S. Reese, J. Waimann, A novel approach for the efficient modeling of material dissolution in electrochemical machining, Int. J. Solids Struct. 229 (2021) 111106. https://doi.org/10.1016/j.ijsolstr.2021.111106
[7] T. van der Velden, S. Ritzert, S. Reese, J. Waimann, Modeling moving boundary value problems in electrochemical machining, accepted in Int. J. Numer. Methods Eng. (2022).
[8] J.L. Pérez-Aparicio, R.L. Taylor, and D. Gavela, Finite element analysis of nonlinear fully coupled thermoelectric materials, Comput. Mech. 40 (2007) 35-45. https://doi.org/10.1007/s00466-006-0080-7
[9] S. Harst, Development of a process signature for electrochemical machining, first ed., Apprimus Wissenschaftsverlag, Aachen, 2019.
[10] J. Waimann, T. van der Velden, A. Schmidt, S. Ritzert, S. Reese, Consideration of chemically-induced damage in a thermo-electrically coupled system, accepted in Proc. Appl. Math. Mech. (2022).